

A thin permeable-membrane device for single-molecule manipulation

Chang-Young Park, David R. Jacobson, Dan T. Nguyen, Sam Willardson, and Omar A. Saleh¹

Citation: *Rev. Sci. Instrum.* **87**, 014301 (2016); doi: 10.1063/1.4939197

View online: <http://dx.doi.org/10.1063/1.4939197>

View Table of Contents: <http://aip.scitation.org/toc/rsi/87/1>

Published by the [American Institute of Physics](#)

A thin permeable-membrane device for single-molecule manipulation

Chang-Young Park,¹ David R. Jacobson,² Dan T. Nguyen,³ Sam Willardson,⁴
and Omar A. Saleh^{5,a)}

¹Materials Research Laboratory, University of California, Santa Barbara, California 93106, USA

²Physics Department, University of California, Santa Barbara, California 93106, USA

³BMSE Program, University of California, Santa Barbara, California 93106, USA

⁴MCDB Department, University of California, Santa Barbara, California 93106, USA

⁵Materials Department and BMSE Program, University of California, Santa Barbara, California 93106, USA

(Received 28 July 2015; accepted 17 December 2015; published online 5 January 2016)

Single-molecule manipulation instruments have unparalleled abilities to interrogate the structure and elasticity of single biomolecules. Key insights are derived by measuring the system response in varying solution conditions; yet, typical solution control strategies require imposing a direct fluid flow on the measured biomolecule that perturbs the high-sensitivity measurement and/or removes interacting molecules by advection. An alternate approach is to fabricate devices that permit solution changes by diffusion of the introduced species through permeable membranes, rather than by direct solution flow through the sensing region. Prior implementations of permeable-membrane devices are relatively thick, disallowing their use in apparatus that require the simultaneous close approach of external instrumentation from two sides, as occurs in single-molecule manipulation devices like the magnetic tweezer. Here, we describe the construction and use of a thin microfluidic device appropriate for single-molecule studies. We create a flow cell of only $\sim 500 \mu\text{m}$ total thickness by sandwiching glass coverslips around a thin plastic gasket and then create permeable walls between laterally separated channels *in situ* through photo-induced cross-linking of poly(ethylene glycol) diacrylate hydrogels. We show that these membranes permit passage of ions and small molecules (thus permitting solution equilibration in the absence of direct flow), but the membranes block the passage of larger biomolecules (thus retaining precious samples). Finally, we demonstrate the suitability of the device for high-resolution magnetic-tweezer experiments by measuring the salt-dependent folding of a single RNA hairpin under force. © 2016 AIP Publishing LLC. [<http://dx.doi.org/10.1063/1.4939197>]

INTRODUCTION

Single-molecule manipulation instruments, such as the optical trap, atomic force microscope, or magnetic tweezer, apply piconewton-scale forces to stretch single biological molecules and use optical tracking techniques to measure the nanometer-scale elastic responses of those molecules.¹ These techniques have proved extremely powerful in the study of various nanoscale biomolecular phenomena, including folding of proteins or nucleic acids and force generation by molecular motor proteins. As with any high-resolution biochemical technique, single-molecule manipulation approaches require careful consideration, and frequently dynamic control, of the solution environment surrounding the measured biomolecule. As such, various authors have integrated microfluidic devices into single-molecule manipulation instruments with the goal of efficiently varying buffer conditions or permitting the controlled introduction of molecules that interact with the studied system.^{2,3} However, prior implementations of such devices require continuous flow conditions, which can waste precious samples by simply advecting them out of the device, and/or create shear forces that perturb the manipulated biomolecule, disrupting the highly sensitive measurement.

A strategy to avoid the deleterious effects of continuous-flow devices but still retain control of sample conditions involves creating permeable membranes that screen the measurement region from direct flow, yet still permit solution changes by diffusion through the membrane. Generally, incorporating permeable membranes within microfluidic devices improves their analytical ability and broadens the range of samples that can be studied by creating protected chambers where the sample can be isolated from hydrodynamic flow. Because of the advantages accrued by avoiding direct flow in the measurement region, permeable-membrane devices have been developed for a variety of soft matter, chemical, or biological studies.^{4–10} However, they have not previously been developed for single-molecule manipulation instruments.

Permeable-membrane devices are generally of one of two design types: the membrane can partition the substrate in either a parallel or perpendicular manner. The former geometry leads to wide channels stacked vertically and separated by a membrane that can potentially be very thin.^{5,7} This has the benefit of a large contact surface and a short diffusion distance between chambers, thereby reducing the equilibration time upon buffer exchange. However, this vertically stacked geometry can cause problems with the high-resolution optical analysis needed for single-molecule measurement: the membrane, which is typically not perfectly transparent, intersects the optical axis, leading to scattering of transmitted light.

^{a)}Electronic mail: saleh@enr.ucsb.edu

The second geometry avoids these problems by using membranes perpendicular to the substrate, thus creating chambers that are horizontally separated.^{4,6} Permeable membranes in this geometry have been fabricated by cross-linking poly(ethylene glycol) diacrylate (PEG-DA) with patterned UV light.⁷⁻¹⁰ This horizontal geometry does not hinder high-resolution optical methods because the membranes do not obstruct transmitted light. Also, with this design, one can easily array several separate lanes; particularly, one can surround a central analysis channel with two flow channels. Flanking lanes allow the reduction of the equilibration time, since the diffusing species can approach from both sides, and permit complex experimental arrangements, such as imposing a solution concentration gradient.^{4,6,8} Additionally, PEG's biocompatibility allows the study of biomolecules or living cells.⁷⁻¹³ However, prior implementations of this device design resulted in flow cells whose vertical thicknesses were too large to permit close approach of external apparatus from both sides. This has precluded their use in instruments that require close access to a sample from both the top and bottom. A notable example of such an instrument is the magnetic tweezer,¹⁴⁻¹⁶ a single-molecule force spectroscopy device that requires the sample to be close to a high-numerical-aperture objective lens on one side and to field-generating rare-earth magnets on the other.

Here, we report the development of a permeable-membrane flow cell with a total thickness, including both capping substrates, of less than 500 μm . The device is made of thin cover slips, a parafilm gasket, thin capillary tubes, and PEG membranes. We demonstrate the semi-permeable nature of the membranes by monitoring the diffusion of ions and small molecules (which pass through the membranes) and of larger DNA constructs (which do not). We then directly test the flow cell by integrating it into a magnetic tweezer. We show that we can resolve nanometer-scale changes in the extension of a single stretched RNA hairpin that are actuated by changing the solution conditions without directly imposing flow.

MATERIALS AND METHODS

Flow cell fabrication

Flow cells were constructed using a three-layered stack of glass cover slips and Parafilm M (Bemis Company). Two cover slips (no. 1, 22×50 and 22×22 mm) were washed with 0.1M NaOH, rinsed with water, and dried with nitrogen gas. The coverslips were further cleaned in a plasma cleaner (PDC-32G, Harrick Plasma) on the high power setting for 5-10 min in 500 mTorr air. Each cover slip was then incubated in a 0.5% solution of 3-(trimethoxysilyl)propyl methacrylate in isopropanol for 1 h at room temperature, rinsed successively with isopropanol and water, and dried with nitrogen gas; this insured good adhesion of the permeable membranes to the cover slips.¹⁷ Parafilm was cut to the size of the square glass slide with a ≈ 4 mm wide internal cutout that would later form the flow channel. The glass slips and parafilm were stacked and fused together by heating with a soldering iron; this created an airtight closure on two sides of the cell.

Permeable membranes were formed by cross-linking PEG-DA under UV illumination through a photomask. PEG-DA (400 Da, Polyscience, Inc.) was pre-mixed with photoinitiator, 2-hydroxy-2-methylpropiophenone (Sigma-Aldrich), in a 50:1 ratio. The solution was diluted with deionized (DI) water to reach a 30% (v/v) PEG-DA solution, vortex mixed and immediately injected into the flow cell. A simple mask was cut from black electric tape using razor blades. The flow cell was then aligned with the razor-cut external mask and exposed to UV light (FOTO/Phoresis, Fotodyne, Inc.; peak emission 300 nm, 0.16 J cm^{-2}) for a period of about 7-10 s. The non-polymerized PEG solution was immediately washed out with DI water. This resulted in a flow cell with three channels: two side channels separated by the PEG membranes from a central channel (Figure 1(c)). The two permeable membranes (PMs) were 300-350 μm in width and the central lane (CL) was about 550 μm wide; these dimensions can be adjusted by varying the photomask dimensions and/or the polymerization time.⁸ Polysulfone capillary tubes (95 μm outer diameter; part no. CTHC074-095-5 from Paradigm Optics) were inserted into ends of the channels and sealed with epoxy. External pumps were connected using Tygon tubing that was inserted over the capillary tubes and sealed with epoxy. Device construction was successful at a rate of roughly 80%; the main hurdle involved the care needed to properly seal the capillary tube/flow cell connection without clogging the capillary with epoxy.

Single-molecule experiment

The RNA hairpin construct was assembled by annealing a 25 base pair (bp) hairpin with a 20 nucleotide (nt) poly(dT) tail to a 828 bp double-stranded DNA handle (see inset of Figure 3(a)); this biomolecular sample geometry was based on that of Dittmore *et al.*¹⁸ The hairpin consisted of the sequence 5'-CUC AGU UGC AAG UGC GAC CUA GGA U-3' connected at the 3' end to its complementary sequence via a hexaethylene glycol spacer. The hairpin and spacer each carried functional groups (biotin and digoxigenin, respectively) that

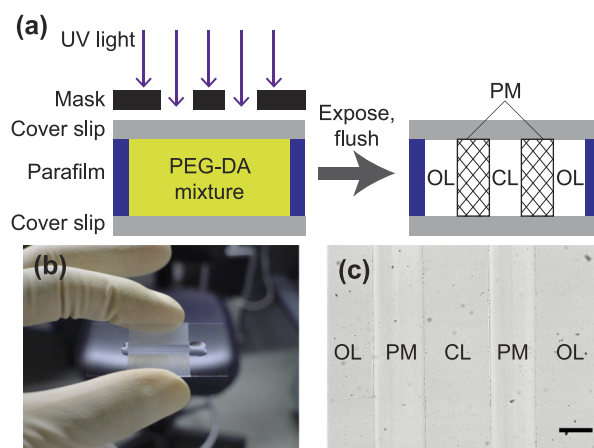


FIG. 1. (a) Sketch of procedure to generate the permeable membrane by exposure of the PEG-DA/photoinitiator solution to masked UV light. (b) Photograph of the completed device. (c) Micrograph of the channels depicting the various components. OL: outer lanes for buffer exchange, CL: central lane for samples, PM: permeable membrane. Scale bar: 250 μm .

permitted attachment to solid surfaces. The interior surfaces of the central lane were functionalized, after membrane fabrication, by incubation with the antibody to digoxigenin (“anti-dig”), which adsorbs to the surfaces. Then, a ~ 100 pM solution of the RNA construct was added to the central lane and allowed to bind to the anti-dig on the surface. Streptavidin-coated magnetic beads (DynaL MyOne C1) were introduced and allowed to bind to the biotin moiety. After flushing to remove unbound beads, the central lane was sealed and a magnet assembly was brought into close proximity to the top surface of the flow cell, applying a force of 11.5 pN to the bead that stretched and destabilized the folded RNA hairpin. Force was calibrated as described previously.¹⁹

RESULTS AND DISCUSSION

We constructed thin flow cells by sandwiching two no. 1 coverslips around a thin Parafilm gasket containing a ~ 4 mm internal channel, and heating to melt the Parafilm, thus creating a tight seal on the edges of the channel. We then synthesized semi-permeable membranes within the channel through the masked photo-polymerization of a PEG hydrogel as depicted in Fig. 1; our protocol is similar to those developed previously.^{7–9,17} Briefly, we mixed PEG-DA with a photo-initiator, injected the solution into the channel, exposed the device to patterned UV light that crosslinked the PEG-DA, and finally flushed with water to remove all unpolymerized solution. The mask pattern resulted in three internal lanes (Fig. 1(c))—a CL flanked on both sides by two outer lanes (OLs), with contact between the lanes mediated by permeation through the hydrogel membranes.

We performed a range of tests to confirm the permeability and biocompatibility of the device. In particular, we measured the permeability of the membranes to a 6.2 kbp (3.7 MDa) plasmid DNA (pTM12), a three-armed “T-DNA”²⁰ construct (38 kDa), the DNA-binding dye YOYO-1 (1.3 kDa), the buffer molecule Tris (121 Da), and the small ions Na^+ and Cl^- (dehydrated weights 23 and 17 Da, respectively).

To measure plasmid DNA and YOYO-1 permeability, we performed a single experiment sensitive to the passage of both species; we added the pTM12 DNA to the central channel and added the YOYO-1 dye to the outer channels. Because YOYO-1 fluoresces strongly only upon intercalation with DNA, fluorescence is only observed if both DNA and YOYO-1 are present. We added the 6.2 kbp plasmid into the central channel at 20 nM concentration, added $100 \mu\text{M}$ YOYO-1 in the outer lanes, then allowed 15 h to elapse (without flow in any lane) to stringently test whether the large DNA molecule could permeate the membrane. After this time, we found that the central lane, and only the central lane, fluoresced, indicating that 1.3 kDa YOYO-1 could pass through the membrane, but that the plasmid could not (Figure 2(a)).

We then tested whether a smaller biomolecule could permeate the membrane, particularly choosing one with similar molecular weight to that of the globular proteins that are frequently the subject of single-molecule analysis. In particular, we utilized a self-assembled T-shaped DNA construct, formed by annealing three single-stranded DNA oligos (Integrated DNA Technologies). Two of the oligos were

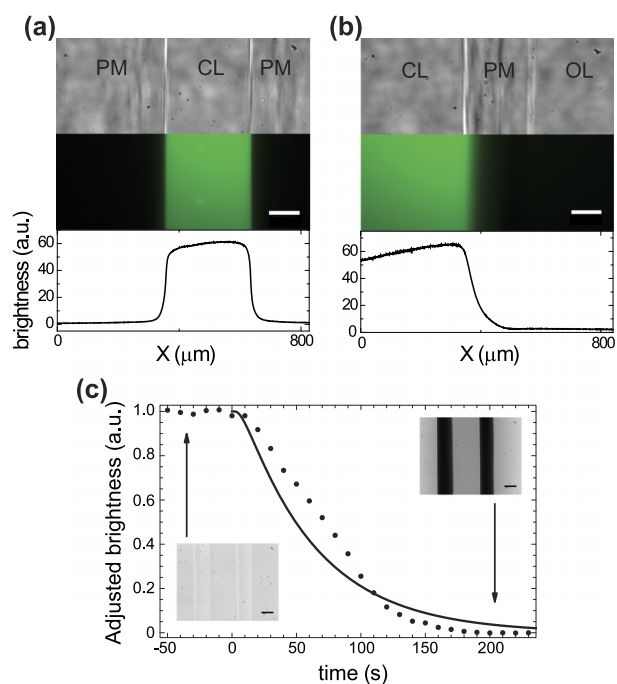


FIG. 2. (a) and (b) Bright-field image, fluorescence image, and fluorescence brightness profile (top to bottom) of the flow cell when filled with fluorescent DNA solutions; scale bars: $100 \mu\text{m}$. In (a), pTM12 was fully confined in the central lane (CL) and YOYO-1 diffused into CL from the outer lane. In (b), the mixture of T-DNA and YOYO-1 was mostly confined in CL, though some of the T-DNA diffused into the membrane (M). There was no evidence of T-DNA in the outer lane. (c) Points: time course of the brightness averaged over the width of the central channel when filled with a bromophenol blue solution during buffer exchange with Tris-HCl. The data have been rescaled along the y-axis to the range (0, 1); the actual brightness dropped by roughly 40% upon equilibration. The line indicates the average concentration in the central channel predicted from the 1-D diffusion equation (Eq. (1)), using a diffusion constant $D = 2.5 \times 10^{-5} \text{ cm}^2/\text{s}$ and assuming a $t = 0$ step-like increase (from zero to a constant value) in the concentration of the diffusing molecule in the side channels. Scale bar: $250 \mu\text{m}$.

40 nt long and one was 47 nt long, with sequence identical to those used by Um *et al.*²⁰ The resulting molecule had a total molecular weight of roughly 38 kDa and consisted of three double-stranded DNA arms, each of length 20 bp. We prepared a flow cell loaded with both $13.3 \mu\text{M}$ T-DNA and $100 \mu\text{M}$ YOYO-1 in the central lane. We again allowed 15 hours for diffusion to occur without flow in the outer lanes. Even after such a long time and with a modestly sized biomolecule, fluorescence was confined to the central channel (Fig. 2(b)). Close inspection revealed that the T-DNA was able to penetrate slightly into the membrane (roughly $100 \mu\text{m}$), but not to pass through. This result demonstrates the ability of the device to confine precious biomolecular samples within the central lane.

Motivated by the goal of studying biomolecular behavior in varying solution conditions, we next investigated the permeation of the common biochemical buffer Tris through the membrane. Tris is not intrinsically fluorescent, so we visualized permeation using the pH sensitive dye bromophenol blue (BPB). BPB, which has an active pH range of 3.0–4.6, imparts on the solution a yellow (blue) color on the acidic (basic) end of the range; here, we measured the yellow-to-blue color change as a darkening on a single-color camera.

A stock solution of BPB was prepared at 0.3 wt. % in DI water and with a pH lower than 3.0, resulting in a yellow solution color. All three flow channels were washed with the stock solution; then, a solution of Tris-HCl (100 mM, pH 7.5) was added to the side channels, and the flow cell was imaged as diffusion of the Tris buffer caused a pH change in the center channel, in turn leading to a full yellow-to-blue transition in the central channel. We also observed a distinctly stronger color in the permeable membranes themselves (insets of Fig. 2(c)), indicating a tendency for BPB to partition into the membranes. Using camera measurements of the transmitted intensity in the central channel, we quantified the kinetics of the color change, finding that the central lane equilibrated in ≈ 200 s (Fig. 2(c)).

We modeled Tris transport using the one-dimensional diffusion equation, in which the time course of Tris concentration follows the relation:

$$\frac{\partial \phi}{\partial t} = D \frac{\partial^2 \phi}{\partial x^2}, \quad (1)$$

where $\phi(x, t)$ is the Tris concentration over time t along the axis x connecting the two side channels and D is the diffusion constant of Tris. This equation was solved numerically in Mathematica to find the Tris concentration, $\bar{\phi}(t)$, averaged across the width of the central channel (as is done with the experimental images). We enforced the boundary conditions that, at $t = 0$, ϕ increases from zero to a constant value in the side channels, at positions $x = \pm 600 \mu\text{m}$, and that the side-channel concentration is constant with time after that increase. For the experiments of Fig. 2, side-channel flow was stopped immediately after Tris was added; in this case, the constant-concentration condition in the side channels is reasonable because of the large size of the side channels relative to the central channel. For certain time scales and flow cell geometries, it might be necessary to add flow to the side channels to stabilize their solution concentrations with time; in that case, the necessary flow rates could be estimated by comparing diffusive and advective time scales for the transported species.

Using a value of $D = 2.5 \times 10^{-5} \text{ cm}^2/\text{s}$, which is consistent with the expectation for a small molecule like Tris, we find that the calculated time course of $\bar{\phi}$ is in reasonably good agreement with the measured darkening of the central channel (Fig. 2(c)). Quantitative deviation of $\bar{\phi}$ from the data is observed; this is likely related to the partitioning effect described above. The success of the diffusion model indicates that ≈ 100 Da molecules such as Tris can easily permeate the membrane and also gives a quantitative basis with which to optimize device parameters such as channel width and flow rate. In particular, these results (along with those shown below) emphasize that the key device parameter is the inter-side-channel distance, controlled here using a relatively basic lithographic scheme. This parameter could be more exactly defined using more advanced lithographic techniques involving, e.g., a photomask and mask aligner.

To fully test the potential of the device in single-molecule experiments and to test the ability of small ions to permeate the membrane, we used magnetic tweezers to measure the mechanical unfolding of a single RNA hairpin while the surrounding salt concentration was changed via diffusion through the membranes. In effect, we leveraged the salt-

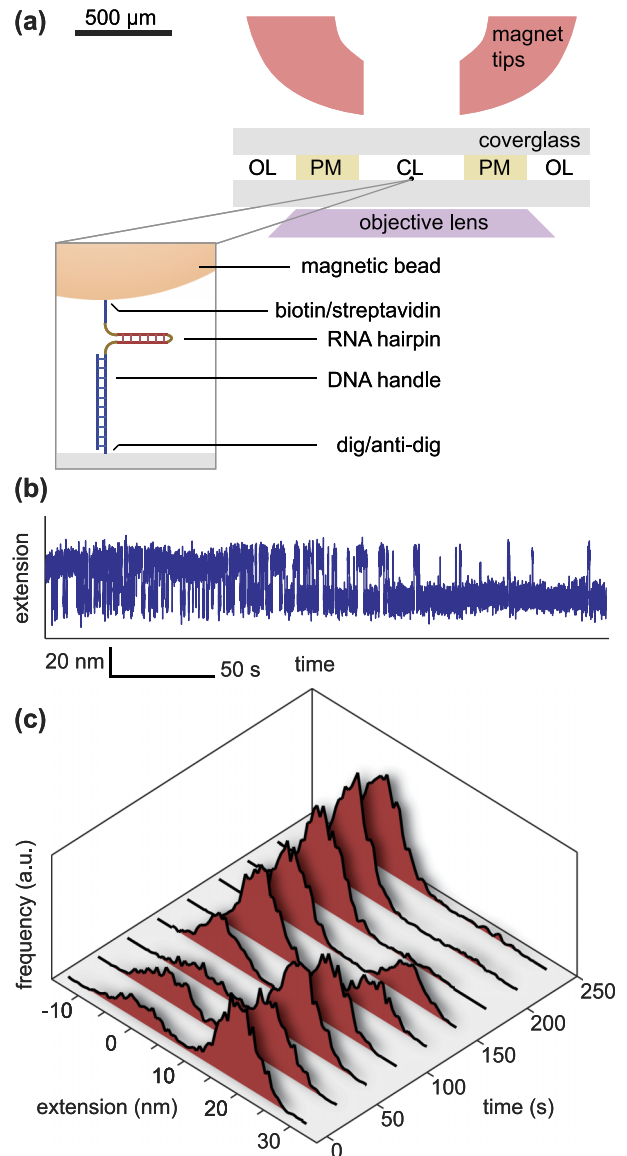


FIG. 3. Demonstration of the thin permeable-membrane flow cell in a single-molecule manipulation experiment. (a) Schematic of the experimental setup, in which the objective lens and magnets must both be brought very close to the sample. Inset not drawn to scale. (b) Extension of the RNA hairpin construct as a function of time as the salt concentration is changed from 10 mM to 100 mM NaCl. (c) Histograms of RNA extension as a function of time (30 s bins) show the transition from the unfolded (high extension and low salt) to the folded (low extension and high salt) state.

sensitivity of nucleic-acid folding to utilize a single RNA molecule as a salt sensor. The experiment is sketched in Figure 3(a). We synthesized a construct containing a 25 bp RNA hairpin attached to a 828 bp DNA spacer and used the construct to tether a magnetic bead to the bottom coverslip within the central channel of a permeable-membrane device. Construct/substrate attachments were achieved using biotin/streptavidin and anti-digoxigenin/digoxigenin interactions for the bead and coverslip, respectively. The device was placed in a magnetic tweezer, in which a magnetic field was applied by bringing a magnet assembly in close vicinity to the upper surface of the flow cell (Figure 3(a)), resulting in a stretching force on the construct that destabilized the folded state of the hairpin. We used particle tracking^{14,15} to measure

the bead height as a function of time, thus reporting on the folded state of the hairpin as solution conditions were altered; particularly, the bead height increases (decreases) when the hairpin unfolds (folds).¹⁸

In initial low-salt conditions (10 mM NaCl), and under 11.5 pN of applied force, we found that the RNA hairpin exhibited stochastic folding fluctuations, but predominantly occupied the extended, unfolded state. While continuously tracking the bead at constant applied force, we then flowed a high-salt solution (100 mM NaCl) through the outer lanes. At higher salt, the screening of RNA's electrostatic self-repulsion is expected to stabilize the folded state.^{18,21} Indeed, over a period of several minutes, we observed changes in the conformational dynamics of the RNA, starting in a mostly unfolded configuration at $t = 0$ s, passing through an equilibrium state with roughly equal time spent in the folded and unfolded states at $t \approx 100$ s, and ending in a mostly folded state at $t \approx 180$ s (see Figures 3(b) and 3(c)). This ≈ 180 s time scale is consistent with the expected result of the 1-D diffusion model: given the diffusion constant of the ions ($D = 1.3 \times 10^{-5}$ cm²/s)²² and the geometry of the device (side channels at positions $x = \pm 500$ μ m), numerical solution to Eq. (1) indicates that the salt concentration will reach 90% of the final value 200 s after the salt change. Further, the measured dynamics were entirely reversible: when flushing low-salt solution through the outer lanes, the dynamic folding behavior went through a reverse process, ending in the same unfolded state as at the beginning. The mean extensions of the hairpin in the low- and high-salt states are consistent with those we have previously observed in a traditional, single-channel flow cell without a membrane.

These results demonstrate the complete compatibility of the flow cell with high-resolution single-molecule analysis, specifically showing (1) that PEG-DA membrane construction had no deleterious effects on the surface chemistry of the device, allowing the use of standard antibody-based methods of biomolecular immobilization; (2) that the device permitted high-resolution particle-tracking-based measurement of biomolecular configuration in a geometry that included closely located magnets; and (3) that the membranes permitted exchange of ionic conditions without affecting the high-resolution measurements; indeed, without any noticeable flow being induced on the single-molecule tether. This last point is in direct contrast to typical magnetic tweezer protocols, where buffer changes require flow through the measurement region that pushes on the tethered bead, disrupting the measurement until flow has stopped and solution conditions have equilibrated. Here, as shown in Figure 3, we are able to track nanoscale biomolecular dynamics during the course of the buffer change.

CONCLUSION

We have demonstrated a thin fluid channel containing biocompatible semi-permeable membranes that is fully compatible with high-resolution single-molecule manipulation in a magnetic tweezer. With the addition of these membranes, the fluidic channel is able to isolate samples and

protect them from shear force while maintaining the ability to control the buffer environment. The horizontal geometry of the channels and membranes prevents any interference with sample imaging. Further, because the flow-cell thickness is only 400–500 μ m, the device can be used in experimental geometries, such as the magnetic tweezer, that require close approach of external apparatus to the flow cell's top and bottom surfaces. We have demonstrated that the membranes have an effective molecular weight cutoff around 5–15 kDa, permitting smaller buffer molecules and ions to pass through the membrane, while retaining larger biomolecules; as shown by prior authors,⁸ we expect tuning of this cutoff to be possible by varying either the length of the PEG-DA used in hydrogel formation or the time of UV curing.

ACKNOWLEDGMENTS

This work was partially supported by NSF Grant No. DMR-1309414 and by the Institute for Collaborative Biotechnologies through Grant No. W911NF-09-0001 from the U.S. Army Research Office. The content of the information does not necessarily reflect the position or the policy of the Government, and no official endorsement should be inferred. C.Y.P. acknowledges partial support from the MRSEC Program of the National Science Foundation under Award No. DMR-1121053. D.R.J. acknowledges support by an NSF graduate research fellowship, No. DGE-1144085.

- ¹K. C. Neuman and A. Nagy, *Nat. Methods* **5**, 491 (2008).
- ²L. R. Brewer and P. R. Bianco, *Nat. Methods* **5**, 517 (2008).
- ³P. Gross, G. Farge, E. J. G. Peterman, and G. J. L. Wuite, in *Methods in Enzymology*, edited by G. W. Nils (Academic Press, 2010), Vol. 475, pp. 427–453.
- ⁴J. Diao, L. Young, S. Kim, E. A. Fogarty, S. M. Heilman, P. Zhou, M. L. Shuler, M. Wu, and M. P. DeLisa, *Lab Chip* **6**, 381 (2006).
- ⁵H. C. Hesse, R. Beck, C. Ding, J. B. Jones, J. Deek, N. C. MacDonald, Y. Li, and C. R. Safinya, *Langmuir* **24**, 8397 (2008).
- ⁶J. Palacci, B. Abecassis, C. Cottin-Bizonne, C. Ybert, and L. Bocquet, *Phys. Rev. Lett.* **104**, 138302 (2010).
- ⁷J. Scrimgeour, J. K. Cho, V. Breedveld, and J. Curtis, *Soft Matter* **7**, 4762 (2011).
- ⁸J. S. Paustian, R. N. Azevedo, S.-T. B. Lundin, M. J. Gilkey, and T. M. Squires, *Phys. Rev. X* **3**, 041010 (2013).
- ⁹M. A. Traore and B. Behkam, *J. Micromech. Microeng.* **23**, 085014 (2013).
- ¹⁰H. Xu, M. M. Ferreira, and S. C. Heilshorn, *Lab Chip* **14**, 2047 (2014).
- ¹¹M. P. Cuchiara, A. C. B. Allen, T. M. Chen, J. S. Miller, and J. L. West, *Biomaterials* **31**, 5491 (2010).
- ¹²D. Castro, P. Ingram, R. Kodzius, D. Conchouso, E. Yoon, and I. G. Foulds, in *2013 IEEE 26th International Conference on Micro Electro Mechanical Systems (MEMS)* (IEEE, 2013), p. 457.
- ¹³V. Hagel, T. Haraszti, and H. Boehm, *Biointerphases* **8**, 32 (2013).
- ¹⁴C. Gosse and V. Croquette, *Biophys. J.* **82**, 3314 (2002).
- ¹⁵N. Ribeck and O. A. Saleh, *Rev. Sci. Instrum.* **79**, 094301 (2008).
- ¹⁶T. Strick, J.-F. Allemand, D. Bensimon, A. Bensimon, and V. Croquette, *Science* **271**, 1835 (1996).
- ¹⁷A. Revzin, R. J. Russell, V. K. Yadavalli, W.-G. Koh, C. Deister, D. D. Hile, M. B. Mellott, and M. V. Pishko, *Langmuir* **17**, 5440 (2001).
- ¹⁸A. Dittmore, J. Landy, A. A. Molzon, and O. A. Saleh, *J. Am. Chem. Soc.* **136**, 5974 (2014).
- ¹⁹B. M. Lansdorp and O. A. Saleh, *Rev. Sci. Instrum.* **83**, 025115 (2012).
- ²⁰S. H. Um, J. B. Lee, N. Park, S. Y. Kwon, C. C. Umbach, and D. Luo, *Nat. Mater.* **5**, 797 (2006).
- ²¹C. V. Bizarro, A. Alemany, and F. Ritort, *Nucleic Acids Res.* **40**, 6922 (2012).
- ²²E. Samson, J. Marchand, and K. Snyder, *Mater. Struct.* **36**, 156 (2003).